Available online at www.sciencedirect.com
SCIENCE DIRECT®
ELSEVIER
International Journal of Solids and Structures 43 (2006) 3794–3816
INTERNATIONAL JOURNAL OF SOLIDS and STRUCTURES
www.elsevier.com/locate/ijsolstr

Dynamic response of anisotropic sandwich flat panels to underwater and in-air explosions

Liviu Librescu [a,*], Sang-Yong Oh [a], Joerg Hohe [b]

[a] *Department of Engineering Science and Mechanics, Virginia Polytechnic Institute and State University Mail Code (0219), Blacksburg, VA 24061-0219, USA*
[b] *Fraunhofer Institut für Werkstoffmechanik, Wöhlerstr. 11, 79104 Freiburg, Germany*

Received 15 March 2005

Abstract

The problem of the dynamic response of flat rectangular sandwich panels subjected to underwater and in-air explosions is analyzed. The study is carried out in the framework of a geometrically non-linear model of sandwich structures featuring anisotropic laminated face sheets and an orthotropic core, in conjunction with the unsteady pressure generated by an explosion. Effects of the core and of the orthotropy of its material, as well as those related to the ply-thickness, directional material property and stacking sequence of face sheets, geometrical non-linearities and of the structural damping ratio are investigated, and their implications upon the dynamic response are highlighted. To the best of the authors' knowledge, the specialized literature addressing the dynamic response of sandwich structures to underwater and in-air explosions is rather scanty. This work is likely to fill a gap in the specialized literature on this topic.

Keywords: Underwater/in-air explosion; Sandwich panel; Dynamic response; Core effects; Face sheet ply-angle

1. Introduction

In modern warfare, naval ships can be exposed to blasts generated by underwater and in-air explosions that can inflict significant damage to their structure. For a reliable structural design of warships against underwater and air-blast, proper expressions of the related blast loading obtained by using fluid-structure

* Corresponding author. Tel.: +1 540 231 5916; fax: +1 540 231 4574.
E-mail addresses: librescu@vt.edu (L. Librescu), sangyong@vt.edu (S.-Y. Oh), hohe@iwm.fhg.de (J. Hohe).

0020-7683/$ - see front matter © 2005 Elsevier Ltd. All rights reserved.
doi:10.1016/j.ijsolstr.2005.03.052

interaction models, and accurate as possible predictions of structural response are required. A good understanding of pertinent factors that decide upon the structural response constitutes an essential pre-requisite toward assessment of the vulnerability and survivability of structures impacted by such explosive pulses. This is valid also for the aeronautical/aerospace structures.

During the last years, for reasons related, among others, to improved fatigue performance, superior energy absorption that yields an increased resistance to impact, reduced susceptibility to corrosion, superior thermal and acoustic insulation, an increased interest for the extensive incorporation of sandwich composites in the construction of naval ships and submarines has been manifested.

This trend was outlined in the extensive review-paper by Mouritz et al. (2001), as well as in the works of the very recent international conference on sandwich constructions, (see the proceedings edited by Vinson et al. (2003)), where the achievements in this area have been presented, and the potential benefits of the incorporation of sandwich composites in the construction of a variety of naval vessels, including the military ones, have been discussed.

In the same sense, the results by Xue and Hutchinson (2004) reveal the superior performance of metal sandwich panels in blast resistant structures, in general, and in water blast, in particular, when comparing with their solid panels counterparts.

The increasing interest in sandwich constructions was reaffirmed also by the appearance of a number of review articles where thorough analyses of the state-of-the-art have been carried out (see e.g. Noor et al., 1996; Abrate, 1997; Vinson, 2001; Frostig, 2003; Hohe and Librescu, 2004).

In the context of the incorporation of sandwich structures in the naval ship constructions, and toward their better design, as one of the necessary requirements, a good as possible understanding of the effects of blasts generated by the underwater and in-air explosions (identified in the sequel by the acronyms, UNDEX and INEX, respectively), and of structural features of sandwich panels on their dynamic response should be reached.

A complexity associated with this issue arises from the fact that the determination of the pressure time-history induced by an underwater explosion acting on a *sandwich panel* involves a more complex analysis than in the case of their monolithic or laminated panel counterparts.

The issue of the dynamic response of sandwich flat panels to time-dependent loads generated by underwater and in-air explosions will be considered in the next developments. In the former case, one supposes that we deal with a submerged panel, while in the latter one, with a topside sandwich panel of ship superstructures, or with a panel of an aeronautical/aerospace sandwich construction. In this context, in order to put into evidence the implications of various non-classical effects, such as those of geometrical non-linearities, initial geometric imperfections, anisotropy of face sheets and their ply-sequence, transverse shear orthotropy properties of the core layer, etc., an advanced model of sandwich constructions will be used. The basic equations of this structural model have been derived in a number of previous papers, (Librescu et al., 1997a,b, 2000).

Having in view the complexity of the dynamic response to explosive blasts, the sandwich model was considered in the context described above, where a number of important features have been incorporated. For the same reasons, the analysis is restricted here to flat panels, only.

One should remark that in the last years a number of highly encompassing models of sandwich and multilayered composite structures have been developed by Vu-Quoc et al. (1997, 2001) and by Vu-Quoc and Ebcioglu (2000a,b) and Vu-Quoc and Tan (2003), respectively, and by Carrera (1998).

It should also be mentioned that with the exception of the works by Moyer et al. (1992), Hayman (1995), Mäkinen (1999a,b), Librescu et al. (2004) and Fleck and Deshpande (2004), where special issues on the dynamic response of sandwich flat panels and beams to underwater explosions have been explored, no other studies on this topic are available in the specialized literature. On the other hand, studies on dynamic response to in-air explosive blasts on standard laminated composite panels have been carried out, among others, by Birman and Bert (1987), Librescu and Nosier (1990) and Vinson (1999).

2. Basic assumptions on the structural model

For the sandwich panel considered in this study, one assumes that the global middle plane is selected to coincide with that of the core layer. Its points are referred to a curvilinear and orthogonal coordinate system $x_\alpha(\alpha = 1, 2)$. The through-the-thickness coordinate x_3 is considered positive when measured in the downward direction. For the sake of convenience, the quantities affiliated with the core layer are identified by a superposed bar, while the ones associated with the bottom and top face sheets are identified by single and double primes, respectively. Consistent with this convention, the uniform thickness of the core is denoted by $2\bar{h}$, while those of the upper and bottom face sheets, as h'' and h', respectively. As a result, $H(\equiv 2\bar{h} + h' + h'')$ is the total thickness of the structure, (see Fig. 1). In this study, symmetric sandwich panels are considered, implying that $h' = h'' \equiv h$, while $a' = a'' \equiv a \equiv \bar{h} + h/2$ is the distance between the global mid-plane of the structure and the mid-planes of the top/bottom face sheets.

The sandwich structural model is based on the following assumptions: (i) the face-sheets are composed of orthotropic material laminae, the axes of orthotropy of the individual plies being rotated with respect to the geometrical axes x_α of the structure, (ii) the material of the core features transverse orthotropic properties, the axes of orthotropy being parallel to the geometrical axes x_α, (iii) the core layer is capable of carrying transverse shear stresses only, and as result we deal with a *weak core*, (iv) a perfect bonding between the face sheets and the core, and between the constituent laminae of the face sheets is postulated, (v) the layers of the face sheets are assumed to be thin; as a result, transverse shear effects in the face sheets, are neglected, (vi) the structure as a whole, as well as both the top and bottom laminated face sheets are assumed to exhibit symmetry properties from both the mechanical and geometrical points of view, with respect to both the mid-plane of the core layer and about their own mid-planes, and finally, (vii) a Lagrangian description of the non-linear model of sandwich structures is adopted in conjunction with the implementation of the von-Kármán non-linear kinematic model and of initial geometric imperfections.

To be reasonably self-contained, in Appendix A, the basic equations of sandwich plate theory incorporating the anisotropy of the individual face sheets and transverse shear effects in the core layer are displayed

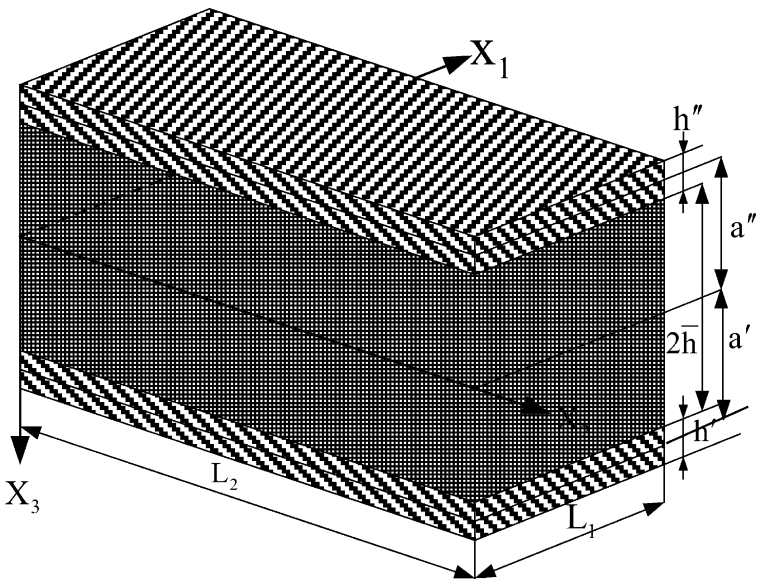

Fig. 1. Geometry of a flat sandwich panel.

only to the extent that they are needed in the treatment and understanding of the subject considered in this paper.

3. Blast loads induced by underwater and in-air explosions

Due to the presence of the core layer, the transmission of pressure waves through the sandwich panel renders the problem of determination of the resultant unsteady pressure more intricate than in the case of the monolithic/laminated panel counterparts. While in the latter case, the theory on which the determination of the pressure time- history on the front face of the panel follows the line established by Kirkwood–Bethe–Cole (see Cole, 1965), in the former case, the ideas developed specifically for the case of a sandwich panels by Hayman (1995), and used subsequently by Mäkinen (1999a,b) will be adopted here.

As it will be seen later, the pressure time-histories based on the previously mentioned structural models feature significant quantitative and qualitative differences that affect the dynamic response of the panel in question. Basically, the unsteady pressure model by Hayman (1995) represents an extension of that devised for a monolithic/laminated panel, in the sense of the inclusion also of the pressure transmitted through the core, reflected at the rear face of the sandwich panel, and then transmitted out into the water.

Having in view the large front of the explosion, the result obtained also by experiments, (see e.g. Houlston et al., 1985), namely that the resulting pressure is uniformly distributed over the plate surface will be adopted also in this study.

As a result, the total pressure in front of the sandwich panel can be represented in the form

$$p_3(t)(\equiv P(t)) = P_i(t) + P_{r1}(t) + P_{r2}(t), \tag{1}$$

where $P_i(t)$ denotes the free-field pressure due to the incident shock wave; $P_{r1}(t)$ is the pressure reflected on the front face, while $P_{r2}(t)$ is the pressure transmitted into the core, reflected at the rear face and transmitted out into the water.

Their expressions are, respectively, as follows:

- $P_i(t) = q_m \mathrm{e}^{-(t-t_1)/\Theta}, \quad t \geqslant t_1,$ (2)

where q_m denotes the peak pressure in the shock front; $t - t_1$ is the time elapsed after the arrival of the shock wave at the panel front surface, Θ is the exponential decay, $t_1 = R/c$, where c denotes the speed of sound in the sea water, while R is the stand-off distance.

For any type of explosive, q_m and Θ are expressed in generic form in terms of Q ($\equiv$ explosive weight [kg]) and R ($\equiv$ the stand-off distance [m]), as

$$q_m = K_1(Q^{1/3}/R)^{A_1} \ (\mathrm{MPa}), \quad \Theta = K_2 Q^{1/3}(Q^{1/3}/R)^{A_2} \ (\mathrm{ms}). \tag{2b,c}$$

As a result, for any specific explosive, constants K_1, K_2, A_1 and A_2 have to be prescribed correspondingly, (see Shin and Geers, 1994; Mäkinen, 1999a,b)

- $P_{r1}(t) = B_1 \mathrm{e}^{-\alpha t} + B_2 \mathrm{e}^{-\beta t},$ (3)

- $P_{r2}(t) = E_1 \mathrm{e}^{-\alpha(t-2\bar{h}/c_\mathrm{c})} + [E_2 + (t - 2\bar{h}/c_\mathrm{c})E_3]\mathrm{e}^{-\beta(t-2\bar{h}/c_\mathrm{c})} + E_4 \mathrm{e}^{-\gamma(t-2\bar{h}/c_\mathrm{c})}.$ (4)

The expressions of the constants appearing in Eqs. (3) and (4) are provided next:

$$\alpha = 1/\Theta, \quad \beta = (\rho c + \rho_\mathrm{c} c_\mathrm{c})/m_\mathrm{f}, \quad \gamma = \rho_\mathrm{c} c_\mathrm{c}/m_\mathrm{f}, \tag{5}$$

where ρ and c are the mass density and speed of sound in the water, respectively, m_f is the mass of the front face sheet per unit area, $c_\mathrm{c}(\equiv \sqrt{E_\mathrm{c}/\rho_\mathrm{c}})$ denotes the speed of sound in the core, where E_c and ρ_c are the Young's modulus and mass density of the core material, respectively. In addition

$$B_2 = \frac{2(\beta-\gamma)q_m}{(\beta-\alpha)}; \quad B_1 = q_m - B_2,$$

$$D_1 = -\frac{2\gamma(\alpha+\gamma)q_m}{(\beta-\alpha)(\gamma-\alpha)}; \quad D_2 = -\frac{2\gamma(\beta+\gamma)q_m}{(\beta-\alpha)(\beta-\gamma)}; \quad D_3 = -(D_1+D_2), \tag{6}$$

$$E_1 = \frac{2(\beta-\gamma)D_1}{(\beta-\alpha)}; \quad E_4 = 2D_3; \quad E_2 = -(E_1+E_4); \quad E_3 = 2(\beta-\gamma)D_2.$$

It should be remarked that the above equations that define the expression of the unsteady pressure apply to both underwater and in-air explosions. However, in the former case the speed of sound and mass density of the sea water at 20 °C are: $c = 1476$ m/s, $\rho = 1009$ kg/m^3, while their in-air counterparts are $c = 330$ m/s and $\rho = 1.20$ kg/m^3. The large differences in the values of c and ρ in sea water and air turn out to have significant implications on dynamic response.

As it will be revealed later, also inclusion of the core effects will bring considerable differences on the pressure and structural time-histories in the two investigated cases of UNDEX and INEX.

In the simulations related to the dynamic response to INEX we are also considering the cases of the sandwich panel impacted by a sonic-boom and a triangular blast. In a compact form, their expressions (see Marzocca et al., 2001) that generalize the specialized ones (Librescu and Nosier, 1990) is

$$P(t) = q_m(1 - t/t_p)[H(t) - \delta_b H(t - rt_p)]. \tag{7}$$

In (7), $H(t)$ denotes the Heaviside step function, δ_b is a tracer that takes the values 1 or 0 depending on whether the sonic-boom or the triangular blast is considered, respectively, t_p denotes the positive phase duration of the pulse measured from the time of impact of the structure, r denotes the shock pulse length factor. For $r = 1$, the sonic-boom reduces to a triangular explosive pulse, while for $r = 2$ it corresponds to a symmetric sonic-boom pulse.

Within the INEX problem we will consider also the tangential blast to the panel surface in the direction of the coordinate x_1 in the form of a traveling-wave

$$P(t) = q_m H(ct - x_1)\exp(-\eta(ct - x_1)), \tag{8}$$

where c is the wave speed in the medium surrounding the structure, while η is an exponent determining the blast decay.

4. Solution methodology

The governing equation system, Eqs. (A.19) and (A.20), in conjunction with the explicit form of the pressure pulse and the boundary conditions have to be solved as to determine the dynamic response of the panel, in terms of displacements η_1, η_2, v_3, and of the Airy's function ϕ.

This constitutes an essential step toward determination of the full response time-history, that involves that of strains and stresses as well. From the mathematical point of view, the problem at hand reduces to the solution of a dynamic non-linear boundary-value problem.

Herein, the sandwich rectangular panel is assumed to be simply supported all over the contour. Consistent with the order (twelve) of the governing system, six boundary conditions have to be prescribed at each edge. Assuming the case of edges unloaded and immovable in the in-plane directions normal to the panel edges, the boundary conditions (see Librescu et al., 1997a,b, 2000), are

$$\xi_1 = 0, \quad N_{12} = 0, \quad \eta_1 = 0, \quad \eta_2 = 0, \quad M_{11} = 0, \quad v_3 = 0 \quad \text{on } x_1 = 0, L_1 \tag{9a–f}$$

and

$$\xi_2 = 0, \quad N_{12} = 0, \quad \eta_2 = 0, \quad M_{22} = 0, \quad v_3 = 0 \quad \text{on } x_2 = 0, L_2. \tag{10a–f}$$

Due to the intricacy of the present boundary value problem, an approximate solution methodology based on extended Galerkin method will be used. In a different context details of this method have been supplied in Librescu et al. (1997a,b).

The conditions expressing the immovability conditions $\xi_1 = 0$ and $\xi_2 = 0$ at $x_1 = 0$, ℓ_1 and $x_2 = 0$, ℓ_2, respectively, are fulfilled on an average sense (see Librescu, 1975; Librescu and Souza, 1993) as

$$\int_0^{L_1}\int_0^{L_2} (\partial\xi_1)/\partial x_1)\,\mathrm{d}x_1\,\mathrm{d}x_2 = 0, \quad \int_0^{L_1}\int_0^{L_2} (\partial\xi_2/\partial x_2)\,\mathrm{d}x_1\,\mathrm{d}x_2 = 0. \tag{11a, b}$$

These conditions in conjunction with the expression of ε'_{11}, ε''_{11} and ε'_{22}, ε''_{22} provided by Eqs. (A.8a) and (A.10a), yield the fictitious edge loads $\underset{\sim}{N}_{11}$ and $\underset{\sim}{N}_{22}$ that render the edges $x_1 = 0$, L_1 and $x_2 = 0, L_2$, immovable.

The expressions of transverse deflection and of initial geometric imperfection satisfying the simple supported boundary conditions are

$$\begin{aligned} &v_3(x_1, x_2, t) = w_{mn}(t)\sin\lambda_m x_1 \sin\mu_n x_2, \\ &\overset{\circ}{v}_3(x_1, x_2) = \overset{\circ}{w}_{mn}\sin\lambda_m x_1 \sin\mu_n x_2, \quad m = 1, 2, \ldots, M; \quad n = 1, 2, \ldots, N, \end{aligned} \tag{12a, b}$$

where $\lambda_m = m\pi/L_1$, $\mu_n = n\pi/L_2$, w_{mn} are the modal amplitudes, L_1 and L_2 are the panel side edges, while $\overset{\circ}{w}_{mn}$ are the model amplitudes of the initial geometric imperfection shape. Moreover, the stress function ϕ is expressed as, (see Librescu, 1975)

$$\phi(x_\omega, t) = \phi_1(x_\omega, t) - \frac{1}{2}(\underset{\sim}{N}_{11}x_2^2 + \underset{\sim}{N}_{22}x_1^2), \tag{13}$$

where $\underset{\sim}{N}_{11}, \underset{\sim}{N}_{22}$ represent the average compressive edge loads, whereas ϕ_1 is a particular solution. Replacing Eqs. (12) and (13) into the compatibility equation (A.19) and solving the resulting non-homogeneous partial differentiation equation yields the expression of ϕ_1 as

$$\phi_1(x_\alpha, t) = A_1(t)\cos 2\lambda_m x_1 + A_2(t)\cos 2\mu_n x_2 - A_3(t)\sin\lambda_m x_1 \sin\mu_n x_2. \tag{14}$$

Similarly, the two coupled equations, namely, Eqs. (A.20a) and (A.20b) can be solved to get

$$\eta_1(x_\omega, t) = B_1(t)\cos\lambda_m x_1 \sin\mu_n x_2, \quad \eta_2(x_\omega, t) = C_1(t)\sin\lambda_m x_1 \cos\mu_n x_2. \tag{15}$$

The coefficients A_i $(i = 1, 2, 3)$ in Eq. (14), as well B_1 and C_1 in Eq. (15) are function of the amplitudes $w_{mn}(t)$ (see Librescu, 1975). These are not recorded here.

Following all the previous steps, replacing the expressions of ϕ, v_3, $\overset{\circ}{v}_3$, η_1,η_2, into the energy functional, Eq. (A.11), and carrying out the indicated integrations results in a non-linear algebraic equation expressed in terms of the modal amplitudes $\delta_{mn}(t)(\equiv w_{mn}(t)/H)$ as

$$P_1[\delta_{mn}, \overset{\circ}{\delta}_{mn}, \underset{\sim}{N}_{11}, \underset{\sim}{N}_{22}] + P_2[\delta_{mn}^2, \overset{\circ}{\delta}_{mn}] = P_{mn}(t) \quad (m = 1, \ldots, M;\ n = 1, \ldots, N). \tag{16}$$

Here P_1 and P_2 are linear and quadratic polynomials in the unknown modal amplitudes whose coefficients depend on the material and geometric properties of the panel; $\overset{\circ}{\delta}_{mn}(\equiv \overset{\circ}{w}_{mn}/H)$ denotes the modal imperfection amplitudes, while $P_{mn}(t)$ are time-dependent functions that are obtained from the previously defined pressure pulses. From Eq. (16) the time-dependent deflection response to specific pressure pulses will be determined, wherefrom the time-dependent response of any quantity of interest, i.e. stress of stress can be obtained.

5. Numerical investigation and results

5.1. Validation of the structural model and of the solution methodology

First of all, in order to validate the performance of the present structural model and the accuracy of the adopted solution methodology, the static response to a lateral uniform pressure, ($p_3 = 100$ kPa), of a geometrically non-linear simply-supported sandwich panel against the results supplied by Riber (1997), are presented in Table 1.

In this context, for the case considered in Riber (1997), the results of an analytical solution and of those obtained via the finite difference method (labelled as FDM), that are supplied in his paper, are compared to the ones obtained by the present structural model via the application of the previously described solution methodology.

As remarked, the agreement with the predictions by Riber (1997) appears to be quite reasonable.

5.2. Results

Unless otherwise stated, the results will be generated by using the material properties listed in Table 2.

Moreover, the results reported here are obtained for a *TNT* explosive. In this case in Eqs. (2)–(6) the following values of the parameters should be considered (see Mäkinen, 1999a,b), $K_1 = 52$; $K_2 = 0.090$ and $A_1 = 1.18$ and $A_2 = -0.18$.

As concerns the architecture of the sandwich wall unless otherwise stated, it follows the rule [0/90/0/90/0/core/0/90/0/90/0].

First of all, it is worthwhile to display the pressure time-histories generated by an underwater explosion, at various distances from the front face of the sandwich panel, by including, (Fig. 2a), and discarding (Fig. 2b) the effects of the transmission of the pressure through the core.

The results emerging from these plots reveal significant qualitative and quantitative differences. Among others: (a) in the case of the inclusion of the core effects, the time at which the cavitation occurs (i.e. the time corresponding to the instant when the resultant pressure becomes a zero-valued quantity), is almost double to that corresponding to the discard of the core effects, (b) whereas in the case of the discard of the core

Table 1
Comparison of maximum response of a sandwich panel subjected to a uniform lateral pressure $p_3 = 100$ KPa

	Displacement (mm)	Bottom face (MPa)		Upper face (MPa)		Core (MPa)	
		σ_{11}	σ_{22}	σ_{11}	σ_{22}	σ_{13}	σ_{23}
Present	10.6	30.1	28.3	−27.1	−25.4	0.62	0.67
Analytical Solution [Riber]	10.4	33.8	30.4	−29.0	−25.3	0.70	0.80
FDM [Riber]	10.0	31.1	28.6	−26.1	−23.0	0.66	0.76

Table 2
Material properties for face sheets and core

Face sheets	Material	E_1 (GPa)	E_2 (GPa)	G_{12} (GPa)	ν_{12}	ρ_f (kg/m^3)
	Graphite/epoxy	207	5.17	2.55	0.25	1588.22
Core	Material	$\overline{G}_{13}$ (MPa)	$\overline{G}_{23}$ (MPa)			ρ_c (kg/m^3)
	PVC foam	11	11			50

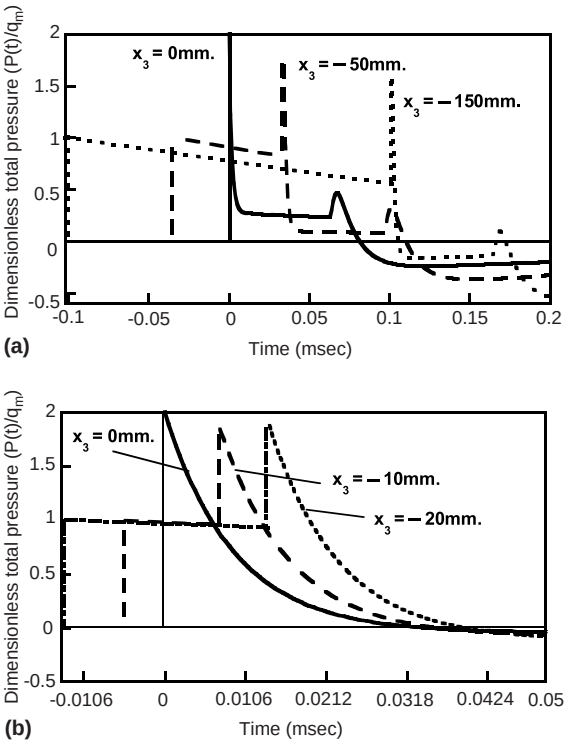

Fig. 2. (a) Dimensionless pressure time-history for various distances from the front panel surface in UNDEX. Effect of the core included ($Q = 30$ kg, $R = 10$ m, $\rho_f/\rho_c = 5$). (b) Counterpart of Fig. 2a when the effect of the core is discarded ($Q = 30$ kg, $R = 10$ m, $\rho_f/\rho_c = 5$).

effects, the cavitation can be expected to occur first at the front panel surface, in the case of the incorporation of the core effects, two cavitation zones are likely to appear, almost at the same time. They are located adjacent to the panel surface, and away from the sandwich front face, in the present case at $x_3 = -150$ mm, and finally, (c) the results supplied in Fig. 2a and b are in excellent agreement with the ones by Hayman (1995) and Mäkinen (1999a,b).

Since the pressure time-history depends not only on the size of the explosive charge and of the stand-off distance, but also on the properties of the sandwich structure, in Fig. 3a and b, the effects of ρ_f/ρ_c on pressure time-history, for the case of the inclusion and discard of the transmission of the pressure through the core are presented. From these plots it appears that in the case of a heavier core (implying the increase of ρ_c), the benefice of a delay of the occurrence of cavitation will occur.

Moreover, for a fixed ρ_f, the increase of ρ_c is accompanied in both cases by an increase of the linear impulse yielding in turn an increase of the severity of the dynamic response.

The results supplied in Figs. 2 and 3 emphasize the fact that incorporation of the effects of the core in the evaluation of the pressure time-history on sandwich construction constitutes an essential requirement for an accurate prediction of their dynamic response, and consequently, of their reliable design.

However, as Fig. 4a reveal, in the case of the INEX, due to the severity of the blast, the inclusion/discard of the core effects does not change the character of the time variation of the blast loading. This implies that the dynamic response of the sandwich panel in an INEX can be carried out by discarding the transmission of the pressure through the core.

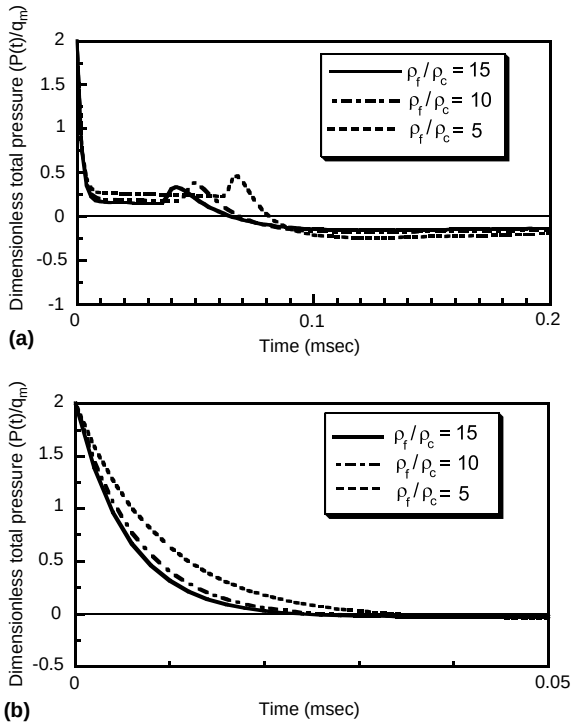

Fig. 3. Normalized pressure time-history on the front face of a sandwich panel due to an UNDEX, in the case of the inclusion of the effects in the core (a) and of their discard (b) ($Q = 30$ kg, $R = 10$ m, $\rho_f = 1528$ kg/m^3).

Fig. 4b displaying the dynamic response to the INEX, reflects in full this fact. Herein, as well as in the next results, the notations have the meaning: $w \equiv \overset{\circ}{v}_3(L_1/2, L_2/2, t) \Rightarrow$ central panel deflection; $\delta_0 \equiv_3 (L_1/2, L_2/2)/H \Rightarrow$ dimensionless central geometric imperfection, while $\zeta \equiv C/2m_0\omega_1 \Rightarrow$ structural damping parameter, where ω_1 is the undamped fundamental frequency of the structural system.

It should be noticed that the character of the pressure time-history in the case of the INEX as emerging from Fig. 4a, appears to be in full agreement with that obtained via experiments by Boyd (2000).

Needless to say, in the case of underwater explosions, the differences in the response predictions in the case of the inclusion/discard of the core effects are significant, and hence, the effects induced by the pressure transmission in the core have to be taken into consideration.

In Fig. 5, the effects of the explosive weight in UNDEX on deflection time-history is presented. It is seen that the increase of Q yields, as expected, an increase of the deflection amplitude. The same is valid when the mass density of the core is increasing.

In this sense, the results of Fig. 6, that are consistent with the trend of variation of the transient pressure for selected values of ρ_f/ρ_c, reveal that the increase of the core density yields an increase of the panel deflection amplitude. It should be noticed that this result is in agreement with the qualitative ones reported by Hayman (1995).

Fig. 7 highlights the effects of the stand-off distance on the deflection time-history to an underwater explosion.

It is seen that with the increase of the stand-off distance there is not only a decrease in the amplitudes of the response, but also a shift of their amplitudes towards larger times.

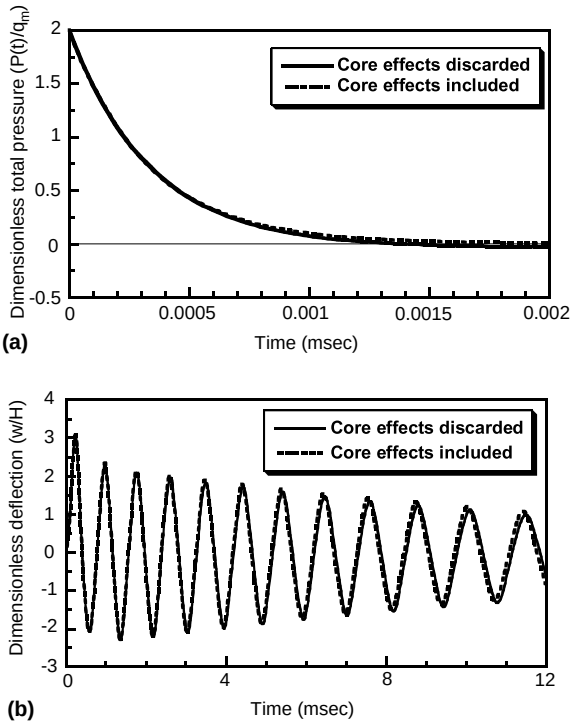

Fig. 4. Pressure time-history on the front face of a sandwich panel due to an INEX (a) and the corresponding dynamic response time-history of the center panel (b) ($L_1/H = 15$, $\delta_0 = 0.05$, $Q = 30$ kg, $R = 10$ m, $\zeta = 0.02$).

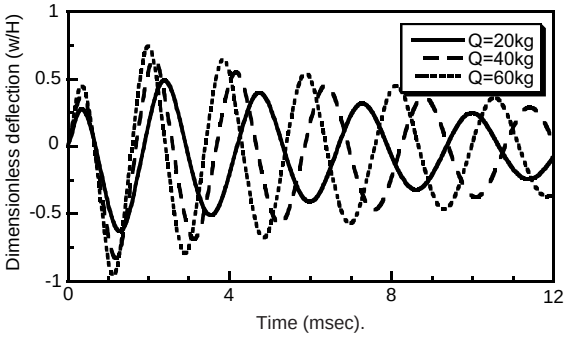

Fig. 5. Effects of the explosive weight on dimensionless deflection time-history of the center of the sandwich panel in UNDEX ($L_1/H = 15$, $\delta_0 = 0.2$, $\zeta = 0.05$, $R = 10$ m).

In Fig. 8 the effects of the thickness of the core layer on the deflection time-history to an UNDEX is presented. It is seen that the increase of the core thickness yields a decrease of oscillation amplitudes, and also a shift of their amplitudes toward larger times. This trend is similar to that reported by Hayman (1995) and Mäkinen (1999a,b).

In Fig. 9 there are shown the effects of the ply-angle of face sheets, for the sandwich panel characterized by the stacking sequence $[\theta/-\theta/\theta/-\theta/\theta/\text{core}/\theta/-\theta/\theta/-\theta/\theta]$.

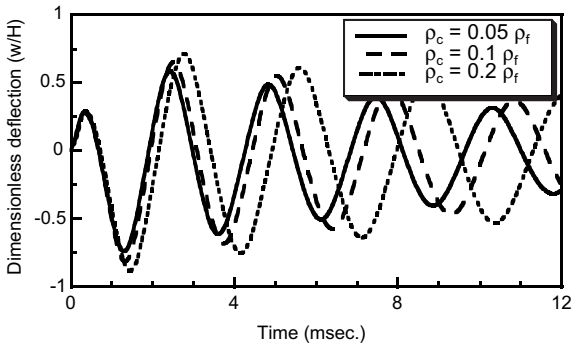

Fig. 6. Effects of relative density of the core on dimensionless deflection time-history of the sandwich panel in UNDEX ($L_1/H = 15$, $\delta_0 = 0.2$, $\zeta = 0.05$, $Q = 30$ kg, $R = 10$ m, $\rho_f = 1528$ kg/m^3).

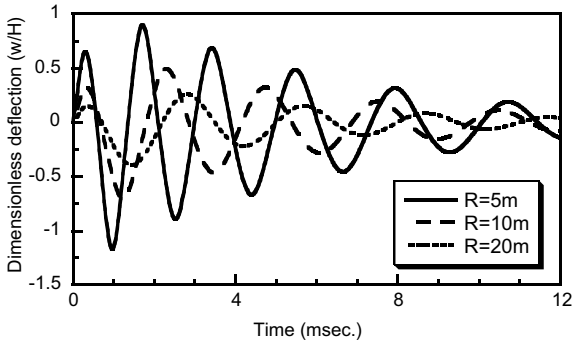

Fig. 7. Effects of the stand-off distance on dimensionless deflection time-history of the center of sandwich panel in UNDEX ($L_1/H = 15$, $\delta_0 = 0.2$, $\zeta = 0.05$, $Q = 30$ kg).

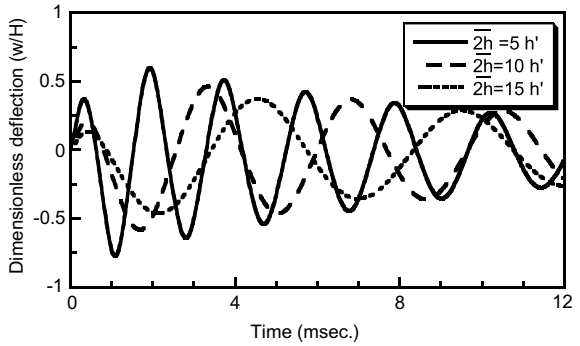

Fig. 8. Effects of the core thickness on dimensionless deflection time-history of the sandwich panel ($L_1/H = 15$, $\delta_0 = 0.2$, $\zeta = 0.05$, $Q = 30$ kg, $R = 10$ m, $h' = 1.9$ mm).

In this case, one considers that the core is orthotropic in transverse shear and that $\overline{G}_{23} = 5\overline{G}_{13}$. The results from this plot reveal that $\theta = 45\,^\circ$ is the best ply-angle from the dynamic response point of view. How-

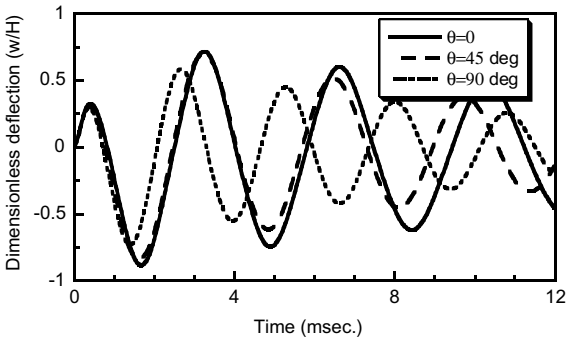

Fig. 9. Effects of ply-angle of face-sheets on dimensionless deflection time-history of the sandwich panel in UNDEX ($L_1/H = 20$, $\delta_0 = 0.2$, $\zeta = 0.05$, $Q = 30$ kg, $R = 10$ m, $\overline{G}_{23}/\overline{G}_{13} = 5$).

ever, the results not displayed here reveal that, depending on the relative value of $\overline{G}_{13}$, different ply-angles can provide an improved dynamic response.

Fig. 10 reveals that the increase of the orthotropicity degree in transverse shear of the core, (measured in terms of the ratio $\overline{G}_{23}/\overline{G}_{13}$), plays a beneficial effect from the dynamic response point of view.

In Figs. 11 and 12, there are shown the effects of the stand-off and weight charge, respectively, on the velocity time-history of the center of the panel subjected to an underwater explosion, while in Figs. 13 and 14, their in-air explosion counterparts are displayed. The values of the velocity response in UNDEX as presented here are in agreement with those report by Jiang and Olsen (1994). The considerable increase of the severity of the in-air explosion as compared to the underwater one that is due to the fact that c and ρ are much lower in the former case than in the latter one, clearly emerges from these plots.

Figs. 6, 8, 11 and 12, have emphasized the significant role played by the stand-off distance and explosive charge on deflection and velocity time-history of the panel central point when subjected to an UNDEX. However, as seen from Figs. 15 and 16, their effect on dimensionless acceleration time-history of the central point of the sandwich structure is really dramatic. For each of considered cases, their peak values have been indicated in the inset of the figures. Notice that the non-dimensionalization of acceleration follows that used by Fagel (1971).

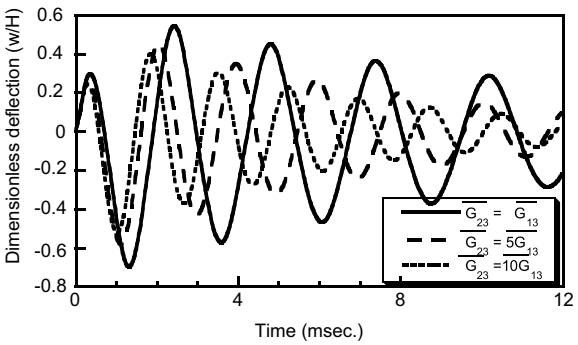

Fig. 10. Effects of orthotropicity degree of the core on dimensionless deflection time-history of the sandwich panel in UNDEX ($L_1/H = 15$, $\delta_0 = 0.2$, $\zeta = 0.05$, $Q = 30$ kg, $R = 10$ m, $\overline{G}_{13} = 11$ MPa).

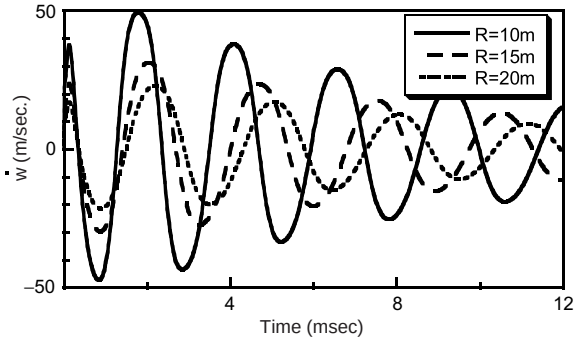

Fig. 11. The effect of the stand-off distance on the velocity time-history of the center of the panel (UNDEX) ($L/H = 15$, $Q = 30$ kg, $\delta_0 = 0.2$, $\zeta = 0.05$).

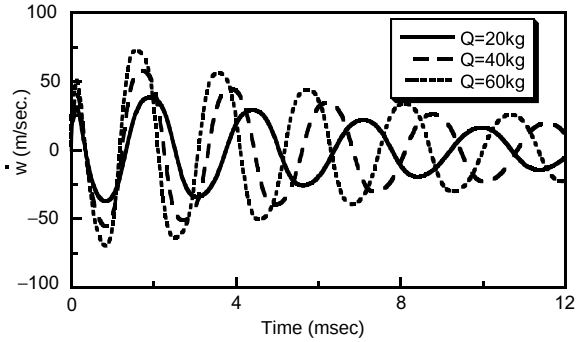

Fig. 12. The effect of the charge weight on velocity time-history of the center panel (UNDEX) ($L/H = 15$, $R = 10$ m, $\delta_0 = 0.2$, $\zeta = 0.05$).

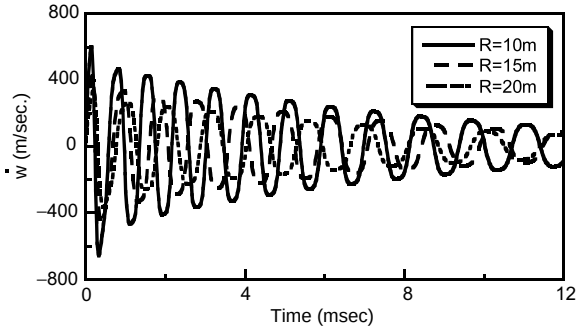

Fig. 13. The counterpart of Fig. 11 for an INEX ($L/H = 15$, $Q = 30$ kg, $\delta = 0.2$, $\zeta = 0.05$).

As is clearly seen, a dimension of the stand-off distance by a factor of two can increase in the same proportion and even more the maximum peak acceleration. However, as time unfolds, the acceleration amplitude, corresponding to various values of R, decay, and also the differences in their amplitudes.

The same trend, but less dramatic appears in connection with the increase of the explosive charge. A similar trend obtained via experiments was reported by Boyd (2000).

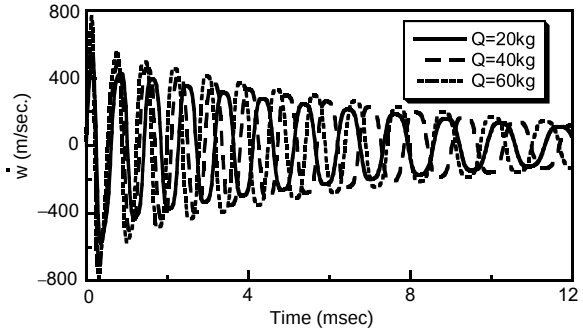

Fig. 14. The counterpart of Fig. 12 for an INEX ($L/H = 15$, $R = 10$ m, $\delta_0 = 0.2$, $\zeta = 0.05$).

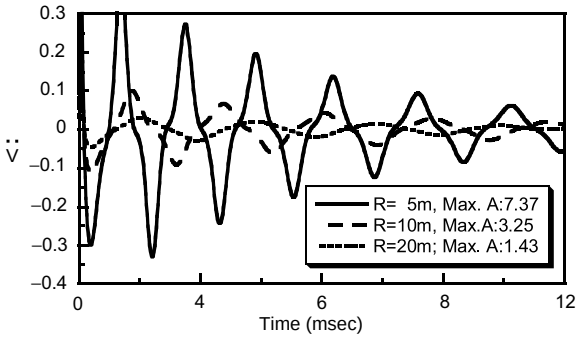

Fig. 15. Effects of stand-off distance on dimensionless acceleration ($\ddot{V} \equiv \ddot{w}/(q_m/m_0)$) time-history of the sandwich center panel (UNDEX) ($L_1/H = 15$, $\delta_0 = 0.2$, $\zeta = 0.05$, $Q = 30$ kg). Their maxima are supplied in the inset.

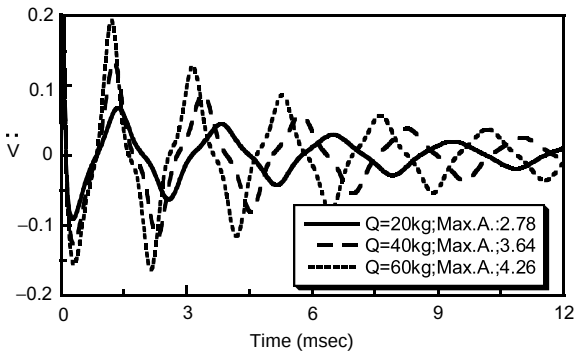

Fig. 16. Effects of the explosive weight on dimensionless acceleration ($\ddot{V} \equiv \ddot{w}/(q_m/m_0)$) time-history of the sandwich center panel (UNDEX) ($L_1/H = 15$, $\delta_0 = 0.2$, $\zeta = 0.05$, $R = 10$ m). Their maxima are supplied in the inset.

In Figs. 17 and 18 there are presented the dimensionless center deflection time-histories of the panel subjected in-air to a tangential shock-wave as influenced by the blast decay η and q_m. The results reveal that the increase of η and of q_m yields a decrease and, respectively, an increase of the response amplitudes.

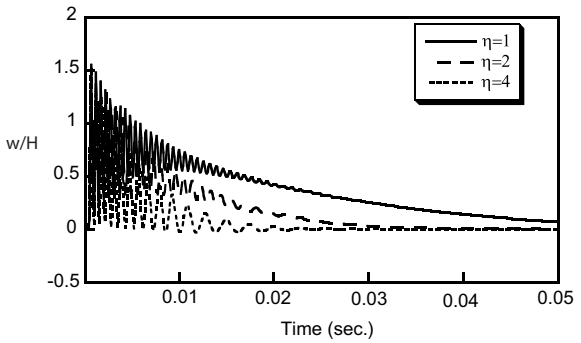

Fig. 17. Effects of decay parameter η of traveling wave on the non-linear dynamic response of the sandwich panel ($L_1/H = 15$, $q_m = 10$ MPa, $\zeta = 0.1$, $\delta_0 = 0.2$, $c = 100$ m/s, $x_1 = 0.1\ L_1$).

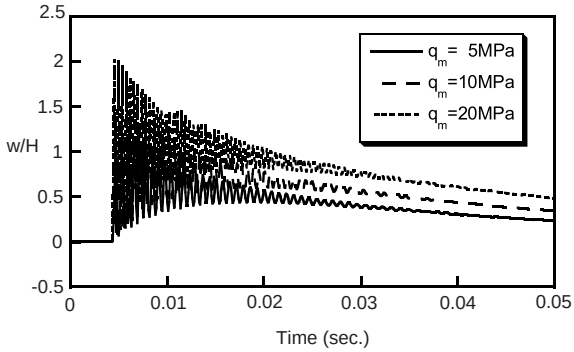

Fig. 18. Effects of the peak pressure of the traveling wave on the non-linear dynamic response of the sandwich panel ($L_1/H = 15$, $\zeta = 0.05$, $\delta_0 = 0.2$, $\eta = 1$, $c = 50$ m/s, $x_1 = 0.5\ L_1$).

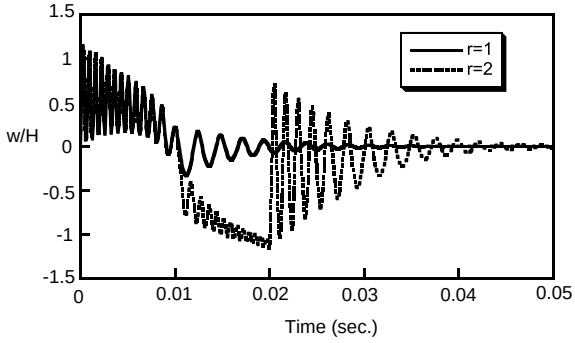

Fig. 19. Non-linear dynamic response of the sandwich panel exposed to triangular/sonic-boom blast ($L_1/H = 15$, $\zeta = 0.05$, $\delta_0 = 0.2$ H, $t_p = 0.01$ s, $q_m = 5$ MPa).

Finally, in Fig. 19 the effects of dimensionless triangular blast ($r = 1$) and of a symmetric sonic-boom ($r = 2$) on the center-panel deflection time-history are presented. It is seen that the sonic-boom pulse yields

a more severe response than the triangular pulse. However, as time unfolds, the difference between the two responses tends to diminish, and finally, to become immaterial.

6. Conclusions

The problem of the dynamic response of geometrically non-linear sandwich flat panels including initial geometric imperfection and subjected to explosive blast loadings produced by both underwater and in-air explosions has been addressed. The implications of a number of structural and geometrical characteristics of the sandwich panel, as well as of the ones related to the respective blasts have been highlighted and related conclusions have been drawn. Consideration of the core effects in the cases of the UNDEX and INEX, has been shown to result in qualitative and quantitative different results, from both the pressure time-history and of the structural response points of view.

The obtained results can be extended without any difficulty as to determine the time-histories of strain and stress components at various points of the sandwich structure. These items are essential toward determining the failure of the structure. Other issues that have still to be addressed are the ones related to the incorporation of the cavitation effects on the dynamic response of submerged sandwich panels exposed to an explosion, and also to the effects played by transverse normal compressibility of the core layer. For such a structural model, see the papers by Hohe and Librescu (2003, 2004). It is hoped that the results supplied here involving the transient response of sandwich structures to underwater and in-air explosions will be instrumental toward a reliable design of naval and aeronautical structures exposed to explosive blasts.

Acknowledgment

This work has been financially supported by the Office of Naval Research (Composites Program) under Grant No. N00014-02-1-0594. The financial support and the interest and encouragement of the Grant Monitor, Dr. Y.D.S. Rajapakse, are gratefully acknowledged.

Appendix A

A.1. Kinematics

Several basic kinematic relationships obtained by specializing for the problem at hand those developed in the monograph by Librescu (1975) and in the paper by Librescu et al. (1997a,b), will be supplied next.

A.1.1. The 3-D displacement field in the face sheets and core

In agreement with the stipulated assumptions, the 3-D distribution of the displacement field fulfilling the kinematic continuity conditions at the interfaces between the core and face sheet results as

$$V'_{\omega}(x_\alpha, x_3) = \xi_\alpha(x_\alpha) + \eta_\alpha(x_\alpha) - (x_3 - a)\partial v_3(x_\alpha)/\partial x_\omega, \quad (\bar{h} \leqslant x_3 \leqslant \bar{h} + h), \tag{A.1a}$$

$$V'_3(x_\alpha, x_3) = v_3(x_\alpha), \tag{A.1b}$$

$$\overline{V}_\omega(x_\alpha, x_3) = \xi_\omega(x_\alpha) + (x_3/\bar{h})\{\eta_\omega(x_\alpha) + (h/2)\partial v_3(x_\alpha)/\partial x_\omega,\}, \quad (-\bar{h} \leqslant x_3 \leqslant \bar{h}), \tag{A.2a}$$

$$\overline{V}_3(x_\alpha, x_3) = v_3(x_\alpha) \tag{A.2b}$$

and

$$V''_{\omega}(x_\alpha, x_3) = \xi_\omega(x_\alpha) - \eta_\omega(x_\alpha) - (x_3 + a)\partial v_3(x_\alpha)/\partial x_\omega, \quad (-\bar{h} - h \leqslant x_3 \leqslant -\bar{h}), \tag{A.3a}$$

$$V''_3(x_\alpha, x_3) = v_3(x_\alpha). \tag{A.3b}$$

In these equations, $V_i(x_\alpha, x_3)$ are the 3-D displacement components in the directions of coordinates x_i. In addition, in the previously displayed equations

$$\xi_\omega = (\widehat{V}'_\omega + \widehat{V}''_\omega)/2; \quad \eta_\omega = (\widehat{V}'_\omega - \widehat{V}''_\omega)/2, \tag{A.3c, d}$$

denote the 2-D average in-plane displacements and half difference of in-plane displacements, respectively, where $\widehat{V}'_\omega$ and $\widehat{V}''_\omega$ denote the in-plane displacements of the points of the mid-planes of the bottom and top face sheets, respectively.

It should be mentioned that in the dynamic case, as considered in this paper, the displacement quantities are functions of time, as well. Although this dependence was not explicitly specified, this is automatically implied.

In the previous and the following equations, the Greek and Latin indices have the range 1, 2, and 1, 2, 3, respectively, and unless otherwise stated, Einstein's summation convention over the repeated indices is employed. In addition, $(\cdot)_{,i}$ denotes partial differentiation with respect to coordinate x_i.

A.2. Distribution of strain quantities across the shell thickness

The structure is assumed to feature a stress-free small initial geometric imperfection $\overset{\circ}{V}_3(\equiv \overset{\circ}{v}_3(x_\alpha))$ that is uniform throughout the panel thickness. Adopting the von-Kármán kinematic approximation in the Green-Lagrange strain tensor that yields,

$$2e_{ij} = V_{i,j} + V_{j,i} + V_{3,i}V_{3,j} + V_{3,i}\overset{\circ}{V}_{3,j} + V_{3,j}\overset{\circ}{V}_{3,i} \tag{A.4}$$

and using (A.4) in conjunction with Eqs. (A.1)–(A.3), one obtains the distribution of 3-D strain quantities $e_{ij}(\equiv e_{ij}(x_1, x_2, x_3))$ across the sandwich wall thickness.

Their expressions are as follows:

In the bottom face-sheets

$$\begin{aligned} e'_{11} &= \varepsilon'_{11} + (x_3 - a)\kappa'_{11}, \quad (1 \rightleftarrows 2) \\ 2e'_{12} &= \gamma'_{12} + (x_3 - a')\kappa'_{12}. \end{aligned} \tag{A.5a, b}$$

In the weak core layer

$$2\bar{e}_{13} = \bar{\gamma}_{13}, \quad (1 \rightleftarrows 2) \tag{A.6}$$

In the top face-sheets

$$\begin{aligned} e''_{11} &= \varepsilon''_{11} + (x_3 + a)\kappa''_{11}, \quad (1 \rightleftarrows 2) \\ 2e''_{12} &= \gamma''_{12} + (x_3 + a'')\kappa''_{12}. \end{aligned} \tag{A.7a, b}$$

The sign $(1 \rightleftarrows 2)$ accompanying the previous and next equations indicates that the expressions of strain quantities not explicitly written can be obtained from the ones that are displayed, by replacing subscript 1 by 2, and vice versa.

In these equations ε_{11}, ε_{22}, $\varepsilon_{12}(\equiv \gamma_{12}/2)$ and $\varepsilon_{13}(\equiv \gamma_{13}/2)$, $\varepsilon_{23} = (\gamma_{23}/2)$ denote the 2-D tangential and the transverse shear strain measures, respectively. Their expressions in terms of the 2-D displacement measures in the face-sheets and core are supplied next.

A.2.1. 2-D strain–displacement relationships

Bottom face sheets

$$\begin{aligned}
\varepsilon'_{11} &= \xi_{1,1} + \eta_{1,1} + \frac{1}{2}v_{3,1}^2 + v_{3,1}\overset{\circ}{v}_{3,1}, \quad (1 \rightleftarrows 2)\\
\gamma'_{12} &= \xi_{1,2} + \xi_{2,1} + \eta_{1,2} + \eta_{2,1} + v_{3,1}v_{3,2} + \overset{\circ}{v}_{3,1}v_{3,2} + v_{3,1}\overset{\circ}{v}_{3,2},\\
\kappa'_{11} &= -v_{3,11}, \quad (1 \rightleftarrows 2)\\
\kappa'_{12} &= -2v_{3,12}.
\end{aligned} \tag{A.8a–d}$$

Weak core layer

$$\bar{\gamma}_{13} = \frac{1}{\bar{h}}\left\{\eta_1 + \frac{1}{2}hv_{3,1}\right\} + v_{3,1}, \quad (1 \rightleftarrows 2) \tag{A.9}$$

Top face sheets

$$\begin{aligned}
\varepsilon''_{11} &= \xi_{1,1} - \eta_{1,1} + \frac{1}{2}v_{3,1}^2 + \overset{\circ}{v}_{3,1}v_{3,1}, \quad (1 \rightleftarrows 2)\\
\gamma''_{12} &= \xi_{1,2} + \xi_{2,1} - \eta_{1,2} - \eta_{2,1} + v_{3,1}v_{3,2} + \overset{\circ}{v}_{3,1}v_{3,2} + v_{3,1}\overset{\circ}{v}_{3,2},\\
\kappa''_{11} &= -v_{3,11}, \quad (1 \rightleftarrows 2)\\
\kappa''_{12} &= -2v_{3,12}.
\end{aligned} \tag{A.10a–d}$$

As a mere remark, due to inclusion of geometrical non-linearities, the stretching-bending coupling is involved in the kinematic equations, Eqs. (A.8)–(A.10).

A.3. Equations of motion and boundary conditions

Hamilton's principle is used to derive the equations of motion and the boundary conditions of geometrically non-linear theory of sandwich flat panels. This may be stated as

$$\delta J = \delta \int_{t_0}^{t_1} (U - W - T)\,\mathrm{d}t = 0, \tag{A.11}$$

where t_0, t_1 are two arbitrary instants of time; U, W and T denote the strain energy, the work done by surface tractions, edge loads and body forces, and the kinetic energy of the 3-D body of the sandwich structure, respectively, while δ denotes the variation operator.

The expressions of U, W and T that can be found in the papers by Librescu et al. (1997a,b) and Hause et al. (1998), are not displayed here.

From (A.11) considered in conjunction with the proper expression of various energy quantities and with the strain–displacement relationships (used as subsidiary conditions), carrying out the integration with respect to x_3 and integrating by parts wherever necessary as to relieve the virtual displacements of any differentiation, and invoking the arbitrary and independent character of the variations $\delta\eta_1$, $\delta\eta_2$, $\delta\xi_1$, $\delta\xi_2$ and δv_3 throughout the entire domain of the plate and within the time interval $[t_0, t_1]$; using the expression of global stress resultants and stress couples (to be defined later), one derive the equations of motion and the boundary conditions associated with the weak core sandwich flat panels.

By retaining only the transversal load, and the transverse inertia and transverse viscous damping, one obtain

The equations of motion:

$$\begin{aligned}
&\delta\xi_1 : N_{11,1} + N_{12,2} = 0,\\
&\delta\xi_2 : N_{22,2} + N_{12,1} = 0,\\
&\delta\eta_1 : L_{11,1} + L_{12,2} - \overline{N}_{13} = 0,\\
&\delta\eta_2 : L_{22,2} + L_{12,1} - \overline{N}_{23} = 0,\\
&\delta v_3 : N_{11}(v_{3,11} + \overset{\circ}{v}_{3,11}) + 2N_{12}(v_{3,12} + \overset{\circ}{v}_{3,12}) + N_{22}(v_{3,22} + \overset{\circ}{v}_{3,22}) + (M_{11,11} + 2M_{12,12} + M_{22,22})\\
&\quad + a/\bar{h}(\overline{N}_{13,1} + \overline{N}_{23,2}) + p_3(x_\alpha, t) = m_0\ddot{v}_3 + C\dot{v}_3,
\end{aligned} \tag{A.12a–e}$$

where C is the transverse viscous damping coefficient, m_0 is the reduced mass per unit area of the panel mid-plane, while the overdots denote time-derivatives.

In addition, *the boundary conditions* that are consistent to the previously displayed equations of motion are as follows:

$$\begin{aligned}
&N_{nn} = \underset{\sim}{N}_{nn} \quad \text{or} \quad \xi_n = \underset{\sim}{\xi}_n,\\
&N_{nt} = \underset{\sim}{N}_{nn} \quad \text{or} \quad \xi_t = \underset{\sim}{\xi}_t,\\
&L_{nn} = \underset{\sim}{L}_{nn} \quad \text{or} \quad \eta_n = \underset{\sim}{\eta}_n \quad \sum\!\!\!\!\!\!\diagup_{n,t},\\
&L_{nt} = \underset{\sim}{L}_{nt} \quad \text{or} \quad \eta_t = \underset{\sim}{\eta}_t,\\
&M_{nn} = \underset{\sim}{M}_{nn} \quad \text{or} \quad v_{3,n} = \underset{\sim}{v}_{3,n},\\
&N_{nt}(v_{3,t} + \overset{\circ}{v}_{3,t}) + N_{nn}(v_{3,n} + \overset{\circ}{v}_{3,n}) + M_{nn,n} + 2M_{nt,t} + (a/\bar{h})\overline{N}_{n3} = \underset{\sim}{M}_{nt,n} + \underset{\sim}{\overline{N}}_{n3} \text{ or } v_3 = \underset{\sim}{v}_3.
\end{aligned} \tag{A.13a–f}$$

In these equations subscripts n and t are used to designate the normal and tangential in-plane directions to an edge and, hence, $n = 1$ when $t = 2$, and vice versa. In addition, the symbol $\sum\!\!\!\!\!\!\diagup_{n,t}$ indicates that no summation over the indices n and t is implied, while the terms underscored by a tilde denote prescribed quantities. It is readily seen that for the present sandwich model of flat panels six boundary conditions should be prescribed at each edge, and consistent with this, a twelfth order governing equation system should result. The displayed equations of motion and static boundary conditions are expressed in terms of the *global* 2-D stress resultants and stress couples

$$\begin{aligned}
&N_{11} = N'_{11} + N''_{11}; \quad N_{12} = N'_{12} + N''_{12}; \quad L_{11} = \bar{h}(N'_{11} - N''_{11}); \quad (1 \rightleftarrows 2)\\
&L_{12} = \bar{h}(N'_{12} - N''_{12}); \quad M_{11} = M'_{11} + M''_{11}; \quad M_{12} = M'_{12} + M''_{12},
\end{aligned} \tag{A.14a–e}$$

where $(N'_{\alpha\beta}, M'_{\alpha\beta})$ $(N''_{\alpha\beta}, M''_{\alpha\beta})$, are the 2-D stress resultants and stress couples measures associated with the lower and upper face sheets, respectively, while $\overline{N}_{\alpha 3}$ are the transverse shear stress resultants associated with the core layer. Their expressions are as follows:

$$\{N'_{\alpha\beta}, M'_{\alpha\beta}\} = \sum_{k=1}^{N} \int_{(x_3)_{k-1}}^{(x_3)_k} (S'_{\alpha\beta})_k \{1, x_3 - a\}\, \mathrm{d}x_3, \tag{A.15a}$$

$$\overline{N}_{\alpha 3} = \int_{-\bar{h}}^{\bar{h}} \overline{S}_{\alpha 3}\, \mathrm{d}x_3 \quad (\alpha, \beta = 1, 2). \tag{A.15b}$$

In Eqs. (A.15) S_{ij} are the components of the second-order Piola-Kirchhoff stress tensor, N is the number of constituent layers in the bottom face sheets, (equal, in the present case, to that in the top faces), whereas $(x_3)_k$ and $(x_3)_{k-1}$ are the distances from the global mid-plane of the structure to the upper and lower interfaces of the kth layer, respectively.

As concerns the 2-D constitutive equations these are provided next.

A.4. Constitutive equation

The constitutive equations associated with the bottom face sheets

$$\begin{aligned} N'_{11} &= A'_{11}\varepsilon'_{11} + A'_{12}\varepsilon'_{22} + A'_{16}\gamma'_{12}, \quad (1 \rightleftarrows 2) \\ N'_{12} &= A'_{16}\varepsilon'_{11} + A'_{26}\varepsilon'_{22} + A'_{66}\gamma'_{12}, \\ M'_{11} &= F'_{11}K'_{11} + F'_{12}K'_{22} + F'_{16}\gamma'_{12}, \quad (1 \rightleftarrows 2) \\ M'_{12} &= F'_{16}K'_{11} + F'_{26}K'_{22} + F'_{66}\gamma'_{12}. \end{aligned} \tag{A.16a–d}$$

The partially inverted form of constitutive equations is obtained from the above equations by solving these for the tangential strains $\varepsilon_{\alpha\beta}$ and of their representation in terms of $N_{\alpha\beta}$. The counterparts of $A'_{\alpha\beta}$ in the representation of $\varepsilon_{\alpha\beta}$ are denoted by $A^{*\prime}_{\alpha\beta}$, where $A^{*\prime}_{\alpha\beta} = A^{*\prime\prime}_{\alpha\beta} \equiv A^{*}_{\alpha\beta}$.

For the soft core layer considered as an orthotropic body (the axes of orthotropy coinciding with the geometrical axes), the pertinent constitutive equations reduce to

$$\overline{N}_{13} = 2\bar{h}\overline{K}^2\overline{Q}_{55}\bar{\gamma}_{13}, \quad \overline{N}_{23} = 2\bar{h}\overline{K}^2\overline{Q}_{44}\bar{\gamma}_{23}, \tag{A.16e, f}$$

where $\overline{Q}_{55} \equiv \overline{G}_{13}$ and $\overline{Q}_{44} \equiv \overline{G}_{23}$ are the transverse shear moduli of the core layer material, while $\overline{K}^2$ is the transverse shear correction factor.

A.5. Governing system

For the problem at hand, the mixed representation of the governing equations is used. This formulation is done in terms of the Airy's potential function ϕ, and the 2-D displacement measures v_3, η_1 and η_2. To this end, by expressing the stress resultants in terms of the Airy's potential function $\phi(\equiv \phi(x_\omega, t))$ as

$$N_{\alpha\beta} = c_{\alpha\omega}c_{\beta\rho}\phi_{,\omega\rho}, \tag{A.16}$$

the equilibrium Eq. (12a,b) are identically fulfilled, where $c_{\alpha\beta}$ denotes the 2-D permutation symbol. Having in view that by virtue of (A.16), the two equilibrium equations (A.12a,b) are eliminated, in order to ensure single valued tangential displacements, the compatibility equation for the tangential strain measures has to be fulfilled.

For flat sandwich panels featuring a weak core this equation is

$$\varepsilon_{11,22} + \varepsilon_{22,11} - \gamma_{12,12} - 2v^2_{3,12} + 2v_{3,11}v_{3,22} + 2\overset{\circ}{v}_{3,11}v_{3,22} + 2v_{3,11}\overset{\circ}{v}_{3,22} - 4v_{3,12}\overset{\circ}{v}_{3,12} = 0, \tag{A.17}$$

where

$$\varepsilon_{11} = \varepsilon'_{11} + \varepsilon''_{11}; \quad \varepsilon_{22} = \varepsilon'_{22} + \varepsilon''_{22}; \quad \gamma_{12} = \gamma'_{12} + \gamma''_{12}. \tag{A.18a–c}$$

Making use of the partially inverted form of constitutive equations considered in conjunction with (A.16), the compatibility equation, Eq. (A.17), can be expressed in terms of the basic unknown functions v_3 and ϕ as

$$A^*_{22}\phi_{,1111} + A^*_{11}\phi_{,2222} - 2A^*_{16}\phi_{,1222} - 2A^*_{26}\phi_{,2111} + (A^*_{66} + 2A^*_{12})\phi_{,1122} - 2v^2_{3,12} + 2v_{3,11}v_{3,22} + 2\overset{\circ}{v}_{3,11}v_{3,22} + 2v_{3,11}\overset{\circ}{v}_{3,22} - 4v_{3,12}\overset{\circ}{v}_{3,12} = 0. \tag{A.19}$$

On the other hand, the equilibrium equations (A.12c-e) represented in terms of displacement quantities and of the Airy's function are

$$A_{11}\eta_{1,11} + A_{16}\eta_{2,11} + A_{66}\eta_{1,22} + (A_{12} + A_{66})\eta_{2,12} + 2A_{16}\eta_{1,12} + A_{26}\eta_{2,22} - (2\overline{K}^2\overline{G}_{13}/\bar{h})(\eta_1 + av_{3,1}) = 0, \tag{A.20a}$$

$$A_{22}\eta_{2,22} + A_{26}\eta_{1,22} + A_{66}\eta_{2,11} + (A_{12} + A_{66})\eta_{1,12} + 2A_{26}\eta_{2,12} + A_{16}\eta_{1,11} - (2\overline{K}^2\overline{G}_{23}/\bar{h})(\eta_2 + av_{3,2}) = 0, \tag{A.20b}$$

$$\phi_{,22}(v_{3,11} + \overset{\circ}{v}_{3,11}) - 2\phi_{,12}(v_{3,12} + \overset{\circ}{v}_{3,12}) - F_{11}v_{3,1111} - F_{22}v_{3,2222} - 4F_{16}v_{3,1112} - 4F_{26}v_{3,1222} - 2(F_{12} + 2F_{66})v_{3,1122} + (2\overline{K}^2 a/\bar{h})\{\overline{G}_{13}(\eta_{1,1} + av_{3,11}) + \overline{G}_{23}(\eta_{2,2} + av_{3,22})\} - m_0\ddot{v}_3 - C\dot{v}_3 + p_3 = 0. \tag{A.20c}$$

In these equations, by virtue of the structural symmetry of the sandwich panel, the stiffness quantities

$$A_{\alpha\beta} \equiv (A'_{\alpha\beta} = A''_{\alpha\beta}), \quad F_{\alpha\beta} \equiv (F'_{\alpha\beta} = F''_{\alpha\beta}), \tag{A.21a, b}$$

whereas the stiffness quantities $A^*_{\alpha\beta}$ represent the inverted counterparts of $A_{\alpha\beta}$.

Herein, for the bottom face sheets

$$\{A'_{\omega\rho}, (\equiv A'_{\rho\omega}); B'_{\omega\rho}(\equiv B'_{\rho\omega}); D'_{\omega\rho}(\equiv D'_{\rho\omega})\} = \sum_{k=1}^{N} \int_{(x_3)_{k-1}}^{(x_3)_k} (\widehat{Q}'_{\omega\rho})_{(k)}(1, x_3, x_3^2)\,\mathrm{d}x_3, \quad (\omega, \rho = 1, 2, 6) \tag{A.21c}$$

and

$$F'_{\omega\rho}(\equiv F'_{\rho\omega}) = D'_{\omega\rho} - 2aB'_{\omega\rho} - a^2A'_{\omega\rho}. \tag{A.21d}$$

For the top face sheets, in Eqs. ((A.21)) the single prime should be changed in double primes and a by $-a$.

By virtue of the symmetry with respect to the global mid-surface of the panel, $\widehat{Q}'_{\omega\rho} = \widehat{Q}''_{\omega\rho}$, where $\widehat{Q}_{\omega\rho}(\equiv \widehat{Q}_{\rho\omega} = Q_{\omega\rho} - Q_{\omega 3}Q_{\rho 3}/Q_{33})$. For more details about the derivation of these equations the reader is referred to Librescu et al. (1997a,b).

References

Abrate, S., 1997. Localized impact on sandwich structures with laminated facings. Applied Mechanical Review 50, 69–82.

Birman, V., Bert, C.W., 1987. Behavior of laminated plates subjected to conventional blast. Journal of Impact Engineering 6 (3), 145–155.

Boyd, S.D., 2000. Acceleration of a plate subjected to explosive blast loading-trial results. Defence Science and Technology, DSTO-TN-0270, Australia.

Carrera, E., 1998. A refined multilayered finite-element model applied to linear and non-linear analyses of sandwich plates. Composites Science and Technology 58, 1553–1569.

Cole, R.H., 1965. Underwater Explosions. Dover Publications, New York.

Fagel, L.W., 1971. Acceleration response of blast-loaded plate. In: Proceedings Shock and Vibration Symposium #42, Shock and Vibration Information Analysis Centre, (SAVIAC), pp. 221–233.

Fleck, N.A., Deshpande, V.S., 2004. The resistance of clamped sandwich beams to shock loading. Journal of Applied Mechanics, Transactions of the ASME 71 (May), 386–401.

Frostig, Y., 2003. Classical and high-order computational models in the analysis of modern sandwich panels. Composites Part B Engineering 34, 83–100.

Hause, T., Librescu, L., Camarda, C.J., 1998. Postbuckling of anisotropic flat and doubly-curved sandwich panels under complex loading conditions. International Journal of Solids and Structures 35, 3007–3028.

Hayman, B., 1995. Underwater explosion loading on foam-cored sandwich panels, sandwich construction, 3, EMAS. In: Proceedings for the Third International Conference on Sandwich Construction, Southampton, England, May 11–15.

Hohe, J., Librescu, L., 2003. A nonlinear theory for doubly curved anisotropy sandwich shells with transversely compressible core. International Journal of Solids and Structures 40, 1059–1088.

Hohe, J., Librescu, L., 2004. Core and face-sheets anisotropy in deformation and buckling of sandwich panels. AIAA Journal 42 (1), 149–158.

Houlston, R., Slater, J.E., Pegg, N., DesRochers, C.G., 1985. On analysis of structural response of ship panels subjected to air blast loading. Computer and Structures 21 (1/2), 273–289.

Jiang, J., Olsen, M.D., 1994. Modeling of underwater shock-induced response of thin plate structures. Report. No. 39, Department of Civil Engineering, University of British Columbia, Vancouver, BC.

Librescu, L., 1975. Elastostatics and Kinetics of Anisotropic and Heterogeneous Shell-type Structures. Noordhoff International Publishing, Leyden, Netherlands.

Librescu, L., Nosier, A., 1990. Response of shear deformable elastic laminated composite panels to sonic boom and explosive blast loadings. AIAA Journal 28 (2), 345–352.

Librescu, L., Souza, M.A., 1993. Postbuckling of geometrically imperfect shear deformable flat panels under combined thermal and compressive edge loadings. Journal of Applied Mechanics, Transactions of the ASME 60, 526–533.

Librescu, L., Hause, T., Camarda, C.J., 1997a. Geometrically nonlinear theory of initially imperfect sandwich plates and shells incorporating non-classical effects. AIAA Journal 35 (8), 1392–1403.

Librescu, L., Meirovitch, L., Na, S.S., 1997b. Control of cantilevers vibration via structural tailoring and adaptive materials. AIAA Journal 35 (8), 1309–1315.

Librescu, L., Hause, T., Johnson, T.F., 2000. Buckling and nonlinear response of sandwich curved panels to combined mechanical loads—implications of face-sheets elastic tailoring. Journal of Sandwich Structures and Materials (2), 246–269.

Librescu, L., Oh, S.-Y., Hohe, J., 2004. Linear and non-linear dynamic response of sandwich panels to blast loading. In: Rajapakse, Y.D.S., Hui, D. (Eds.). Composites B. Special Issue on Marine Composites 35 (4–5), 395–424.

Mäkinen, K., 1999a. Underwater shock loaded sandwich structures. Department of Aeronautics, Royal Institute of Technology, Report 99-01, Stockholm, Sweden.

Mäkinen, K., 1999b. The transverse response of sandwich panels to an underwater shock wave. Journal of Fluids and Structures 13, 631–646.

Marzocca, P., Librescu, L., Chiocchia, G., 2001. Aeroelastic response of 2-D lifting surfaces to gust and arbitrary explosive loading signature. International Journal of Impact Engineering 25 (1), 67–85.

Mouritz, A.P., Gellert, E., Burchhill, P., Challis, K., 2001. Review of advanced composite structures for naval ships and submarines. Composite Structures 53, 21–41.

Moyer Jr., E.T., Amir, G.G., Olsson, K.A., Hellbralt, S.E., 1992. Response of GRP sandwich structures subjected to shock loading. In: Second International Conference on Sandwich Construction, B1-B17, University of Florida, Gainsville, FL, March 9–12.

Noor, A.K., Burton, W.S., Bert, C.W., 1996. Computational models for sandwich plates and shells. Applied Mechanical Review 49, 155–199.

Riber, H.J., 1997. Non-linear analytical solutions for laterally loaded sandwich plates. Composite Structures 39 (1-2), 63–83.

Shin, Y.S., Geers, T.L., 1994. Response of marine structures to underwater explosions. International Short Course Notebook, Shock and Vibration Research, Monterey, CA.

Vinson, J.R., 1999. The Behavior of Sandwich Structures of Isotropic and Composite Material. Technomic Publications Co., Inc., Lancaster, Basel.

Vinson, J.R., 2001. Sandwich structures. Applied Mechanical Review 54, 201–214.

Vinson, J.R., Rajapakse, Y.D.S., Carlsson, L.E. (Eds.), 2003. 6th International Conference on Sandwich Structures. CRC Press, Boca Raton, London, New York, Washington, DC.

Vu-Quoc, L., Ebcioglu, I.K., 2000a. General multilayer geometrically-exact beams and one-dimensional plates with deformable layer thickness. Zeitschrift für Angewandte Mathematik und Mechanik (ZAMM) 80 (2), 113–135.

Vu-Quoc, L., Ebcioglu, I.K., 2000b. Multilayer shells: Geometrically-exact formulation of equations of motion. International Journal of Solids and Structures 37 (45), 6705–6737.

Vu-Quoc, L., Tan, X.G., 2003. Optimal solid shells for nonlinear analyses of multilayer composites. Part II: Dynamics. Computer Methods in Applied Mechanics and Engineering 192 (9–10), 1017–1059.

Vu-Quoc, L., Ebcioglu, I.K., Deng, H., 1997. Dynamic formulation for geometrically-exact sandwich shells. International Journal of Solids and Structures 34 (20), 2517–2548.

Vu-Quoc, L., Deng, H., Tan, X.G., 2001. Geometrically-exact sandwich shells: The dynamic case. Computer Methods in Applied Mechanics and Engineering 190 (22–23), 2825–2873.

Xue, Z., Hutchinson, J.W., 2004. A comparative study of impulse-resistant metal sandwich plates. International Journal of Impact Engineering 30, 1283–1305.